Elsevier Editorial System(tm) for Journal of Chromatography A

Manuscript Draft

Manuscript Number:

Title: Rationale behind the optimum efficiency of columns packed with new 1.9 µm fully porous particles of narrow particle size distribution.

Article Type: Full Length Article

Keywords: Column efficiency, Sub-2µm fully porous particles of narrow particle size distribution (nPSD), Mass transfer, Eddy dispersion

Corresponding Author: Prof. Alberto Cavazzini, PhD

Corresponding Author's Institution: University of Ferrara

First Author: Martina Catani

Order of Authors: Martina Catani; Alberto Cavazzini, PhD; Omar H Ismail; Alessia Ciogli; Claudio Villani; Luisa Pasti; Caterina Bergantin; Deirdre Cabooter; Gert Desmet; Francesco Gasparrini; David S Bell

Suggested Reviewers: Attila Felinger
felinger@ttk.pte.hu
Expert of the field

Peter Schoenmakers
p.j.schoenmakers@uva.nl
Expert of the field

Fabrice Gritti
fabrice_gritti@waters.com
Expert of the field

Opposed Reviewers: Ulrich Tallarek Prof.
See cover letter. Our feeling is that prof. Tallarek was reviewer-2 of JCA-15-1392. His very long revision had some personal comments that were really rude and disrespectful of our work and professionalism.

UNIVERSITY OF FERRARA
Department of Chemistry and
Pharmaceutical Sciences

UNIVERSITÀ DEGLI STUDI DI FERRARA
- EX LABORE FRUCTUS -

Via L. Borsari 46, 44121 Ferrara, Italy
Fax:+39-0532-240709

Dear Editor,
We are pleased to submit two papers regarding the study of the kinetic performance of columns packed with new 1.9 micron fully porous particle of narrow particle size distribution (nPSD). These columns are commercially known with the name of Titan C18. The first reports on these columns have evidenced their really impressive kinetic performance with efficiency in larger than 300,000 theoretical plates per meter under typical reversed-phase conditions and this attracted the interest of the scientific community.

Last summer we submitted a paper about this subject to JCA. The paper JCA-15-1392 was rejected on Sept. 1st. In that work, we suggested that the great performance of these columns was due to their very small eddy dispersion term (A term of the van Deemter equation). This idea was in contrast with the results published, with the same columns, by Gritti and Guiochon (Gritti and Guiochon, J. Chromatogr. A 1355 (2014) 179–192; Gritti and Guiochon, J. Chromatogr. A 1355 (2014) 164–178). Gritti and Guiochon indeed demonstrated that the origin of the efficiency of these columns was the extremely reduced intraparticle diffusion.

The two papers we are submitting now represent a complete revision and extension of JCA-15-1392 with a lot of new information and experimental data. Not only, we have performed additional experiments by employing different compounds (in addition to alkyl benzenes already employed in JCA-15-1392), but also we have accurately and independently evaluated all terms of the van Deemter equation (by following essentially the same approach of Gritti and Guiochon in J. Chromatogr. A 1355 (2014) 179–192).

The first paper, titled “Experimental evidence of the kinetic performance achievable with columns packed with new 1.9 μm fully porous particles of narrow particle size distribution”, reports on the characterization of a relevant number (six) of columns of different geometries to point out their great kinetic performance. This work gives evidence that these nPSD columns can be efficiently operated at relatively large flow rates, which is contrast with the hypothesis of low intraparticle diffusion as the origin of the great kinetic performance of these columns. The second work, “Rationale behind the optimum efficiency of columns packed with new 1.9 μm fully porous particles of narrow particle size distribution”, presents a fundamental study of mass transfer in these nPSD columns. The single terms of van Deemter equation were evaluated independently by applying the most advanced methodologies nowadays available.

The most important conclusion that we can draw from these new measurements confirms our first supposition that the excellent performance of these nPSD comes from a very small eddy dispersion term, while the B and C terms of the van Deemter equation are comparable to those of other columns packed with particles of similar geometry and chemistry.

Obviously, in writing these two papers, we have carefully considered all the comments by the three reviewers of JCA-15-1392. For instance, as reviewer-1 advised, we performed new experiments by employing the same phenone derivatives used by Gritti and Guiochon in their study. This was indeed important and it evidenced a quite different behavior from that observed by Gritti and Guiochon that was at the basis of their explanation of the origin of the great efficiency of these columns due to the very small intraparticle diffusion. As reviewer-2 and 3 pointed out, we measured the single terms of the van Deemter equation through an experimental protocol that includes peak parking, pore blocking and ISEC. This approach allows for the independent and very accurate estimation of the A, B and C term of van Deemter equation.

As a conclusive note, we would like to ask to avoid that reviewer-2 of JCA-15-1392 be one of the reviewers of these papers. While we can accept all scientific comments and we are really open to that, we believe that what this reviewer wrote was not respectful of our work. As an example, expressions such as “slow motion suicide” should not be used to comment on the scientific work of other people.

With best regards,
Alberto Cavazzini
Francesco Gasparrini

Highlights

► New sub 2μm C18 fully porous particles with narrow particle size distribution (nPSD)

► Kinetic performance of nPSD columns is studied from a theoretical viewpoint

► Excellent kinetic performance comes from very small eddy dispersion term

► B- and C-term of van Deemter equation similar to those of fully porous C18 columns

Rationale behind the optimum efficiency of columns packed with new 1.9 μm fully porous particles of narrow particle size distribution.

Martina Catani[a], Omar H. Ismail[b], Alberto Cavazzini[a,*], Alessia Ciogli[b], Claudio Villani[b], Luisa Pasti[a], Caterina Bergantin[a], Deirdre Cabooter[c], Gert Desmet[d], Francesco Gasparrini[b], David S. Bell[e]

[a]*Dept. of Chemistry and Pharmaceutical Sciences, University of Ferrara, via L. Borsari 46, 44121 Ferrara, Italy*
[b]*Dept. of Drug Chemistry and Technology, "Sapienza" Università di Roma, P.le A. Moro 5, 00185 Roma, Italy*
[c]*KU Leuven, Department of Pharmaceutical Sciences, Pharmaceutical Analysis, Herestraat 49, Leuven 3000, Belgium*
[d]*Vrije Universiteit Brussel (VUB), Department of Chemical Engineering, 1050 Brussels, Belgium*
[e]*Applied Research and Development, Millipore Sigma, 595 North Harrison Road. Bellefonte, PA 16823, USA*

Abstract

Columns packed with new commercially available 1.9 fully porous particles of narrow particle size distribution (nPSD) are characterized by extremely high efficiency. Under typical reversed phase conditions, these columns are able to generate very high number of theoretical plates (in the order of 300,000 plates/meter and more). In this paper, we investigate the origin of the high performance of these nPSD columns by performing a series of measurements that include, in addition to the traditional determination of the van Deemter curve, peak parking, pore blocking and inverse size exclusion experiments. Two nPSD columns (both 100×3.0 mm) have been considered in this study: the first one, packed with particles of 80Å pore size, is commercially available. The second one is a prototype column packed with 1.9 fully porous particles of 120Å pore size.

The main conclusion of our study is that these nPSD columns are characterized by extremely low eddy dispersion, while longitudinal diffusion and mass transfer kinetics are substantially equivalent to those of other fully porous particles of similar chemistry.

Keywords: Column efficiency, Sub-2μm fully porous particles of narrow particle size

*Corresponding author
Email address: cvz@unife.it (Alberto Cavazzini)

1. Introduction

In the companion paper to this one [1], the kinetic performance of columns packed with the recently introduced 1.9 μm fully porous particles (average pore diameter 80Å), known with the commercial name of Titan C_{18}, has been investigated by using a series of benzene derivatives under reversed phase (RP) conditions. The study was performed on a set of 6 columns (length: 50, 75 and 100 mm, internal diameter 2.1 and 3 mm) that represents, in our opinion, a large enough sample to draw reliable conclusions on their kinetic behaviour. The most relevant results from that study confirmed, on the one hand, the excellent kinetic performance of narrow particle size distribution (nPSD) columns already demonstrated in literature [2, 3] (with reduced HETP, h, as small as 1.7-1.9) but, on the other hand, revealed how these columns can be very efficiently operated even at relatively large flow rates [1]. This latter conclusion thus contrasts those of Gritti and Guiochon [2, 3] who observed, by using a series of phenone derivatives under RP conditions, a dramatic loss of performance when the column was operated at velocities slightly larger than the optimum. Gritti and Guiochon explained this finding on the base of the very low intraparticle diffusivity that would characterize the Titan C_{18} particles (about three times smaller, for a retention factor of 2, than for typical fully porous C_{18} particles). Following [2, 3], the unusually low intraparticle diffusivity not only explains the very good performance of these columns at relatively low flow rates (thanks to very reduced longitudinal dispersion) but also their scarce performance at high flow rates due to slow mass transfer [2, 3]. On the other hand, no effect on eddy dispersion was observed.

In this study we present a detailed investigation of contributions to band broadening of the individual steps involved in the migration of the compound peaks through heterogeneous porous media. Essentially the same experimental protocol as in [2, 3] was employed. It requires peak parking [4–7], total pore-blocking [8, 9] and accurate HETP measurements. Combined with models of effective longitudinal diffusion through the

packed bed [10–12], this information permits to achieve a physically-sound interpretation of mass transfer in modern liquid chromatography (LC) columns. Even though the main study was performed by using a series of benzene derivatives as probe compounds, for the sake of comparison the van Deemter curves of phenone derivatives used in [2, 3] were also investigated.

Finally, besides the Titan C_{18} column packed with 1.9 μm fully porous particles with average pore size 80Å used in previous works [1–3], a prototype column (supplied by Supelco) was also fully characterized from a kinetic viewpoint. This column is packed with Titan C_{18} 1.9 μm but of average pore size 120Å

2. Theory

Under the hypothesis of independence of the different contributions leading to peak broadening in LC [13, 14], the functional relationship between the reduced plate height $h = H/d_p$ (being H the HETP and d_p the particle diameter) and the interstitial reduced velocity ν is commonly written as the sum of four terms including the eddy dispersion, $a(\nu)$, the longitudinal diffusion, b/ν, the external mass transfer resistance, $c_m\nu$, and the mass transfer resistance across the stationary phase, $c_s\nu$ [15, 16], that is:

$$h = a(\nu) + \frac{b}{\nu} + c_m\nu + c_s\nu \tag{1}$$

The interstitial reduced velocity is defined as:

$$\nu = \frac{u_e d_p}{D_m} \tag{2}$$

where D_m is the bulk molecular diffusion coefficient and u_e is the interstitial velocity, i.e. the velocity referred to the mobile phase moving between particles [17]:

$$u_e = \frac{F_v}{\pi r_c^2 \epsilon_e} \tag{3}$$

being F_v the flow rate, r_c the inner column radius and ϵ_e the external column porosity:

$$\epsilon_e = \frac{V_e}{V_{col}} \tag{4}$$

with V_{col} the geometric volume of the column.

For columns packed with very fine particles, usually a term accounting for the frictional heating due to the stream of the mobile phase against the bed under significant pressure must be added to Eq. 1. However, given the quasi-adiabatic conditions under which experiments were performed, it was not necessary to add this term [18–21].

The meaning of the different terms appearing in Eq. 1 is well known. The longitudinal (or axial) diffusion term describes the band broadening due to the diffusion of molecules through the porous particles and the interstitial volume in absence of flow. Since this is the only contribution to band broadening when the flow is switched off, it is best estimated through peak parking experiments [4–7]. In reduced coordinates, the longitudinal diffusion term b is given by [5, 13, 15, 22]:

$$b = 2(1 + k_1)\frac{D_{eff}}{D_m} = 2(1 + k_1)\gamma_{eff} \tag{5}$$

where D_{eff} is the effective longitudinal diffusion coefficient, γ_{eff} ($= D_{eff}/D_m$) is the dimensionless effective diffusion coefficient and k_1 is the zone retention factor, defined as [5, 23]:

$$k_1 = \frac{t_R - t_e}{t_e} \tag{6}$$

being t_R the retention time and t_e the time spent by a species molecule in the interstitial volume. k_1 is connected to the more often employed phase retention factor, k, via:

$$k_1 = \frac{(1 + k)\epsilon_{tot}}{\epsilon_e} - 1 \tag{7}$$

where ϵ_{tot} ($= V_0/V_{col}$, being V_0 the thermodynamic void volume) is the total column porosity. The interpretation of D_{eff} is traditionally done in terms of the so-called Knox parallel-zone model (or residence time weighted model) [5, 13, 24], where D_{eff} is given by:

$$D_{eff} = \frac{t_e D_m \gamma_e + t_{ms} D_m \gamma_{ms} + t_s D_s \gamma_s}{t_e + t_{ms} + t_s} \tag{8}$$

being t_{ms} and t_s the time spent by a molecule in the stagnant mobile phase (inside particles) and in the stationary phase, respectively, while γ_e, γ_{ms}, γ_s are the obstruction factors

for the interstitial, stagnant and solid zone. The assumption at the base of Eq. 8 is that diffusion inside and outside the particles are independent processes. However Desmet and coworkers [10, 11] demonstrated that these two processes cannot be treated separately, due to the presence of different competitive mechanisms, characterized by different rate parameters, which simultaneously contribute to the process of diffusion of a molecule from two points in the packed structure [14, 25]. A more physically-sound description of diffusion through complex composite porous media, therefore, can be obtained by employing the Effective Medium Theory (EMT) [26]. Among the many EMT models available in literature, the simplest is Maxwell's expression of the effective longitudinal diffusion in fully porous ordered and random sphere packings is written as [10, 11, 15, 27–30]:

$$D_{eff} = \frac{1}{\epsilon_e(1+k_1)}\left[\frac{1+2(1-\epsilon_e)\beta}{1-(1-\epsilon_e)\beta}\right]D_m \tag{9}$$

where β is the so-called polarizability constant:

$$\beta = \frac{\alpha_{part}-1}{\alpha_{part}+2} \tag{10}$$

and α_{part} is the relative permeability:

$$\alpha_{part} = \frac{D_{part}K_p}{D_m} \tag{11}$$

where D_{part} is the overall diffusion coefficient through the porous particles (including diffusion in the stagnant mobile phase and surface diffusion) and K_p is the whole-particle volume (V_{part})-based equilibrium constant, that is:

$$K_p = \frac{m/V_{part}}{C_m} \tag{12}$$

where m and C_m represent the mass of the adsorbed species and the equilibrium concentration in the mobile phase, respectively. Therefore, operatively, K_p can be calculated by:

$$K_p = \frac{k_1\epsilon_e}{1-\epsilon_e} \tag{13}$$

The simple Eq. 9 has been proven to be accurate (5%) over the entire range of diffusion and retention conditions [12, 28, 29].

The kinetic c_s term appearing in Eq. 1 describes the mass transfer across the stationary phase. Since there is absence of flow inside particles, the mass transfer coefficient across the stationary phase is velocity-independent, which makes it easier to establish theoretically-sound expression for this contribution [16]. Following Giddings [13], for fully porous spherical particles this term is commonly expressed as [15, 22]:

$$c_s = \frac{1}{30}\frac{k_1}{(1+k_1)^2}\frac{D_m}{D_{part}} \tag{14}$$

On the contrary, the estimation of the external-film mass transfer coefficient c_m (see Eq. 1) is very complex and the best approximations currently existing for this term are poorly accurate [15, 31]. Usually in LC the semi-empirical correlations obtained by Wilson Geankoplis and by Kataoka [32] are employed for the estimation of c_m, which were however measured with particles having much larger diameters ($\simeq$6.2 mm) than those nowadays in use [33].

Finally, the eddy dispersion term, $a(\nu)$ in Eq. 1, is caused by the erratic flow profile in the through-pores of the packed bed. It includes trans-channel eddy dispersion, short-range inter-channel eddy dispersion, trans-column eddy dispersion. Despite the fundamental work of Giddings culminated in the well-known coupling theory [13], there is still considerable debate in literature regarding the values of the geometrical parameters needed to describe the complex structures of packed beds [34]. Much work in this direction has been done by Tallarek's group with a very sophisticated approach based on the morphology reconstruction of the actual stationary phase structure and the calculation of transport properties in the reconstructed materials [35–38]. On the other hand, an experimental estimation of $a(\nu)$ can be achieved by subtracting to accurately measured h values (Eq. 1) both the longitudinal diffusion and the mass transfer terms independently estimated by Eqs. 5 and 14 [15]:

$$a(\nu) = h - \frac{b}{\nu} - c_s\nu \tag{15}$$

(For the reasons given above, in this paper, the external mass transfer contribution c_m will not be counted in the subtraction. This means that Eq. 15 returns a slight overestimation of $a(\nu)$).

3. Experimental section

Columns and materials. Two 100×3.0 mm (length×internal-diameter) stainless steel Titan C_{18} columns packed with 1.9 μm particles of respectively 80Å and 120Å pore size were employed. C_{18} ligand density was 2 μmol/m^2 for the 80Å column (specific surface area 400 m^2/g) and 3 μmol/m^2 for the 120Å one (specific surface area 300 m^2/g). The columns were generously donated by Supelco Analytical (USA). Polystyrene standards (molecular weights 500, 2000, 2500, 5000, 9000, 17500, 30000, 50000, 156000, 330000, 565000, 1030000, 1570000, 2310000) employed for Inverse Size Exclusion measurements were purchased from Supelco. Decane, 2-propanol, tetrahydrofuran, uracil, phenol, nitrobenzene, benzaldehyde, benzene, toluene, ethylbenzene, butylbenzene, propylbenzene, pentylbenzene were from Sigma-Aldrich. Acetonitrile (ACN) was from VWR International. Ultra-high quality Milli-Q water was obtained by a Milli-Q water purification system (Millipore).

Equipment. A Waters Acquity UPLC, controlled by Empower 3 software and equipped with a binary solvent delivery system, an autosampler, a column thermostat, a photodiode array detector with a 500 nL cell, was used for the determination of the van Deemter curves. The equipment was operated under still-air [21, 39] and quasi-adiabatic conditions. The maximum back pressure reachable by the system is 1,000 bar. To reduce the extra-column contributions, two 250×0.075 mm nano-Viper capillary tubes (Thermo Scientific) were used to connect, respectively, the injector to the column and the column to the detector. The extra column peak variance, measured from the injector needle port to the detector cell, was 1.2 μL^2 (calculated through peak moments) at a flow rate of 1 mL/min. ISEC experiments were carried out on an Agilent 1100 Series Capillary LC system equipped with a binary pump system, an autosampler, a column thermostat (Peltier unit) and a photodiode array detector. This equipment was also employed for peak parking experiments.

Inverse size exclusion chromatography (ISEC). ISEC measurements were performed by using tetrahydrofuran as the mobile phase [40]. Injection volume, flow rate and detection

wavelength were, respectively, 2 μL, 0.1 mL/min and 254 nm. Retention volumes were corrected for the extra-column contribution before being plotted against the cubic root of the molecular weight. As shown in [1], the (ISEC estimation of) external column volume, V_e, is calculated by extrapolating the excluded branch of this plot. The thermodynamic void volume, V_0, was calculated from the corrected elution volume of benzene in tetrahydrofuran.

Total Pore Blocking. The external column volume was also estimated by using the so-called total pore blocking method [8, 41]. In this case, columns were firstly flushed with 100 mL of 2-propanol and then with 60 mL of decane to fill with it the pores of the stationary phase. Finally, pure water was used to remove decane from interstitial space of columns. Complete removal of decane was confirmed by monitoring both DAD signal and column backpressure and by repeatedly injecting an unretained molecule (thiourea dissolved in pure water) until a constant elution volume was achieved, which gives (the total pore blocking estimation of) V_e. Columns were flushed again with 2-propanol to remove the blocking agent from the pores before further use.

Peak parking measurements. The flow rate used for peak parking measurements was 0.1 mL/min. Parking times were 0, 120, 600, 1800 and 3600 s. For the calculation of the variance (in length units) of the eluted peak, σ_x^2:

$$\sigma_x^2 = L^2/N \tag{16}$$

where L is the column length, the number of theoretical plates N was calculated by the integration tool of the software. All the data were corrected for the extra-column peak variance, calculated as the second central moment of the peak fitted through an exponentially modified Gaussian (EMG) function [42].

Van Deemter curve measurements. The van Deemter curves for nitrobenzene, toluene, ethylbenzene and butylbenzene were measured at 35.0$\pm$0.1°C. The mobile phase was a binary mixture of ACN/water 60:40 v/v. The injection volume was 0.5 μL. Retention time and

column efficiency (N) of eluted peaks were automatically calculated by the Empower software (v. 3). The detection wavelength was 214 nm; sampling rate was 80 points/s. Due to the very reduced extra-column volume of the modified Waters UPLC employed in this work (see before for details), no correction was applied to compensate for the extra-column contribution. The flow rates employed for studying the dependence of H on the mobile phase velocity were 0.025, 0.05, 0.1 ml/min and then, from 0.1 ml/min to the maximum reachable flow rate, step increments of 0.1 ml/min were applied (see figure captions for more information).

SEM measurements. SEM images of both bare-silica and C_{18}-functionalized Titan C_{18} particles were obtained with a Zeiss EVO 40. The instrument was operate with an accelerating voltage of 20 kV and with 5000$\times$ magnification. Particles were conductive enough to omit the use of carbon coating. Of every particle batch, the diameter of at least 500 particles was measured. To determine particle sizes, SEM pictures were uploaded in a drawing program (Windows Paint) and straight lines, corresponding to the diameter of particles, were manually drawn over them. This manual procedure was preferred because it allowed determining the position of particle circumference with the highest possible degree of precision and certainty. The length of straight lines was determined in an automated way using an in-house written script in Imaq Vision Builder (National Instruments Corporation, Austin, TX, USA). d_{Sauter} was calculated as:

$$d_{Sauter} = \frac{\sum_{i=1}^{n} n_i d_i^3}{\sum_{i=1}^{n} n_i d_i^2} \tag{17}$$

where d_i and n_i are, respectively, a given particle size and the number of particles with diameter included between d_i and $d_i + \Delta d_i$. Δd_i was assumed 0.07.

The particle size distribution of the different supports was subsequently determined from the nominal particle sizes, by expressing the diameter of at least 500 particles per column batch in a frequency distribution diagram. To properly normalize the graph (surface under curves should be unity), the results were plotted as $(d_{ave} \times n_i) / \sum(n_i \times \Delta d_i)$ vs. d_i / d_{ave}, being d_{ave} the average particle diameter.

4. Results and discussion

Geometric characteristics of Titan columns employed in this work are compared in Table 1 (experimental details on these measurements are given in [1]). ϵ_e was estimated by both ISEC and total pore blocking experiments. The agreement between the two techniques was within about $\pm 3\%$ (in Table 1, only the ISEC-based estimations of ϵ_e have been reported). It is worth to notice how experimental values of ϵ_e (0.364 and 0.369, respectively for the 80 and the 120 Å column) are very close to the theoretical limit (0.36) calculated by Baranau and Tallarek [43] for frictionless random-close packings of particles with a PSD similar to that of the Titan C_{18} columns (about 10%) [1]. This confirms that packing of columns has been extremely efficient. ϵ_e is one of the most important parameters controlling the quality of columns, inasmuch as both hydrodynamic dispersion and hydraulic permeability strictly depend on it. Not surprisingly, therefore, specific permeabilities of columns (Table 1, sixth column) were also very similar (plots of column backpressure vs. mobile phase velocity needed for the estimation of k_0 are reported under Supporting Information).

The van Deemter curves measured on the two columns are given in Figure 1 in the form of H vs. u_e. Four compounds were considered in this work, nitrobenzene, toluene, ethylbenzene and butylbenzene. They cover a wide range of retention factors going from 2.7 to more than 20 if given as zone retention factor k_1 (see Table 2, columns 2-3) or from 1.2 to 12.3, if expressed as phase retention factor k (see Table 2, columns 4-5 and Eq. 7). Two important things can be evidenced by these curves. The first one is the excellent kinetic performance of both columns, with H values at the minimum of the van Deemter curves (H_{min}) significantly lower than twice the particle diameter, traditionally taken as a "reference" value for well-packed fully porous particle columns [17]. This is especially evident for the Titan C_{18} 120Å column. Calculated as the average of the minimum heights obtained for the four compounds, indeed, H_{min} was 3.7 μm for the Titan C_{18} 80Å column (at u_e roughly 0.65 cm/s) and only 3.3μm for the Titan C_{18} 120Å one (u_e approx. 0.7 cm/s). The second interesting aspect is that, up to maximum achievable velocity (back-pressure

reachable by the system is max 1,000 bar), van Deemter curves for all compounds on both columns are very flat. Therefore, Titan C_{18} columns can be employed at (relatively) large flow rates, without losing perfomance. As a visual proof of the excellent performance of these columns, in Figures 2 and 3 the chromatograms for the separation of a mixture of benzene derivatives (including phenol, benzaldehyde, nitrobenzene, benzene, toluene, ethylbenzene, propylbenzene, butylbenzene, pentylbenzene), whose retention factors range from 1 to almost 24, are reported: some 300,000 and 320,000 N/m were measured on the Titan C_{18} 80Å and the Titan C_{18} 120Å column, respectively (see figure captions for details).

A more quantitative measure of column performance can be obtained by plotting the van Deemter curves in reduced coordinates. d_{Sauter}-based reduced van Deemter curves are shown in Figure 4. Following [2], in these plots, d_{Sauter} was assumed equal to 2.04 μm. Impressive reduced h_{min}s were observed. For instance, h_{min} as small as 1.65 (at ν_{opt} = 5.5) and 1.52 (at ν_{opt}=6.1) was obtained with nitrobenzene (k = 1.3), respectively on the Titan C_{18} 80Å and the Titan C_{18} 120Å column. h_{min} and ν_{opt} for all the compounds considered in this work are reported in Table 2 (columns 5-8).

From the data reported in the last two columns of this table, one may also appreciate how the efficiency of columns is substantially maintained at the largest velocities reached in this work. For instance, by considering ethylbenzene ($k_1 \simeq 8.0$), h changes by only about 1%, on the Titan C_{18} 80Å column, going from ν_{opt} (8.4) to the maximum velocity ν_{max} = 10.6 and by less than 1%, on the Titan C_{18} 120Å one, passing from ν_{opt} = 7.6 to ν_{max} = 9. Even though the compounds employed for measuring column performance are different (benzene- vs. phenone-derivatives), this example allows for a qualitative comparison with the work by Gritti and Guiochon [2, 3] who obtained, on a Titan C_{18} 80Å column (100×3 mm) under RP conditions for a compound with comparable retention (octaphenone, k_1 = 10.2), very similar h_{min} (1.7) but at a significantly lower optimal velocity ν_{opt} = 5. Contrary to us, in addition, they observed a dramatic loss of efficiency by slightly increasing the flow rate over the optimum value. As it was already mentioned before,

the explanation proposed by Gritti and Guiochon [3] to explain this behavior is that C_{18} fully porous Titan particles are characterized by an unusually low (if compared to other particles of similar geometrical characteristics and chemistry) intraparticle diffusivity. To further compare our results with those of Gritti and Guiochon, we therefore performed a series of van Deemter curve measurements by using the same set of phenone derivatives employed in [2, 3] (acetophenone, propiophenone, butyrrophenone, valerophenone, hexanophenone) as probe compounds. The detailed results of this study are given as Supplementary Information. Enough to say here that the performance of columns with phenones were substantially similar to those with benzene derivatives (e.g., on the Titan C_{18} 80Å column, the average H_{min} calculated on the five phenones was 3.25 at u_e = 0.45, vs. average H_{min} = 3.7 at u_e = 0.65 for benzene derivatives, see before). In addition, we could not observe the same loss of performance, by increasing the flow rate over its optimum value, as reported in [2, 3].

For the sake of comparison between different packing porous particles used in LC, the Titan C_{18} 80Å column was emptied and particles were subjected to SEM analysis. After elaboration of SEM images (reported under Supplementary Information), PSD and d_{Sauter} of Titan C_{18} 80Å particles were calculated as described under the Experimental section. In Figure 5, the normalized PSD of Titan C_{18} 80Å particles is represented together with those of some common fully porous and superficially porous particles (see figure caption for details), whose PSD was calculated in the same manner in [44]. From this figure, it is evident that Titan particles have an extremely narrow PSD, even comparable to those of superficially porous particles (which are well known for being characterized by nPSDs) and significantly narrower than those of other common fully porous particles. A strong (nearly linear) correlation between the width of the PSD and the a-term of the van Deemter equation has been previously observed [44] and could indicate that the excellent performance and low reduced a-terms observed for the Titan particles in this study are a consequence of their excellent packing structure. On the other hand, application of Eq. 17 to SEM image of Titan C_{18} 80Å particles returned d_{Sauter} = 2.4 μm. By recalculating h_{min}

and ν_{opt} based on this value, an average h_{min} (calculated on the four compounds) of 1.56 at ν_{opt} = 8.16 was obtained.

In the following, the single terms of the van Deemter equation on Titan C_{18} columns will be independently evaluated by following an approach based on the combination of stop-flow experiments and the EMT-based Maxwell's model (Eq. 9) for the interpretation of diffusion through porous media. For the calculation of the b-term, the knowledge of the apparent or effective axial diffusion coefficient D_{eff} is required (Eq. 5). As it was detailedly described in [1] (but for the estimation of the bulk molecular diffusion D_m), D_{eff} can be estimated by the slope of the plot reporting the variance of the eluted peak against the time the peak was left to diffuse inside the Titan C_{18} columns without flow (parking time). One example of such a plot is given in Figure 6. D_{eff} and b coefficients for the compounds considered in this work are reported in Table 3. As it can be seen from these data, in all cases, b represents roughly 35-40% of h_{min}, which is the typical value for modern columns packed with fully porous particles [12, 45]. On the other hand, b-terms estimated in this work are some 15% larger than those reported by Gritti and Guiochon for Titan C_{18} 80Å columns in [3, 46] (at comparable k_1).

According to the EMT, the correct driving force for diffusion in presence of preferential solubility (such as in LC) is the gradient in chemical potential and not the gradient in concentration. Accordingly, the correct property obeying EMT-rules is the permeability and not the diffusivity [10]. The calculation of the relative permeability, α_{part}, can be easily performed from Eqs. 11 and 10 since β can be unequivocally measured from Eq. 9 (being D_{eff}, ϵ_e, k_1 and D_m known). α_{part} values are reported in Table 3. α_{part} corresponds to the so-called sample intraparticle diffusivity, Ω, of [3, 46]. Therefore, following what is usually done in literature [12, 46], these values can be expressed as a function of k_1 and compared each others. This comparison, whose results are graphically given under Supporting Information, has evidenced that α_{part}s measured in this work are about 30% larger than values given in [46].

The next step is the estimation of D_{part}, which can be done by means of Eq. 11, once

K_p (Eq. 13) is known (see Table 3, columns 8-11). Interestingly, for all benzene derivatives, D_{part} was found about 20% larger on the Titan C_{18} 120Å column than on the 80Å one. The faster the intraparticle mass tranfer, the smaller the c_s term (Eq. 14) of the van Deemter equation. Indeed, Table 3 (columns 12-13) shows how c_ss on the Titan 120Å column are about 20% smaller than those measured on the 80Å one. In terms of c_s coefficient, the comparison between our data and those obtained by Gritti and Guiochon [46] with a similar Titan C_{18} 80Å column shows that c_s-terms measured in this work are about 25-30% smaller than those obtained for phenones of comparable k_1.

Finally, the information in our possess permits to estimate $a(\nu)$ by difference between h and the independent estimates of b and c_s (Eq. 15). Figure 7 shows how $a(\nu)$ changes with ν for the two Titan C_{18} columns. $a(\nu)$ was calculated as the average of the values obtained for the four compounds. As it can be seen, eddy dispersion term presents the typical asymptotic behavior already reported by other authors, e.g. [15, 47]. However, on the Titan columns, $a(\nu_{max})$ is remarkably small. Indeed at $\nu_{max} \simeq 10$, its value is only 1.2 on the Titan C_{18} 80Å column and even 1.0 on the Titan C_{18} 120Å one. In Table 4, eddy dispersion values (at $\nu \simeq 10$) taken from literature for different fully porous and core-shell commercial particles are reported. These data point out the very small eddy dispersion of Titan C_{18} columns, particularly for the Titan C_{18} 120Å one, whose a-term is very close to that of core-shell Kinetex 2.6 μm particles [48]. Figure 7 also shows that, by increasing the flow rate, $a(\nu)$ increases less on the 120Å column than on the 80Å one, but it is very difficult to provide a physically-sound explanation to these experimental findings. In a recent study, it was observed that the inner particle morphology of a packing also has a significant effect on the dispersion [49]. The combination of nPSD and differences in pore size of the 80Å and 120Å could hence provide an explanation for the observed differences in eddy dispersion, that are anyhow very small in both cases.

5. Conclusions

A detailed investigation of mass transfer processes on two nPSD Titan C_{18} columns, by employing a series of benzene derivatives as test compounds, has revealed that these

columns are characterized by an extremely small eddy dispersion, even comparable to those of columns packed with core-shell particles. On the other hand, contrary to previous conclusions, the b and c_s terms of the van Deemter equation were found to be essentially comparable to those of other columns packed with particles of similar chemistry and characteristics. Our findings therefore do not confirm the previous hypothesis that the extraordinary efficiency of these nPSD columns is generated by a very small intra-particle diffusion. These conclusions were further supported by the investigation of the behavior of phenone derivatives under reversed phase conditions.

6. Acknowledgments

The authors thank the Italian University and Scientific Research Ministry (Grant PRIN 2012ATMNJ_003) and the Laboratory Terra&Acqua Tech, member of Energy and Environment Cluster, Technopole of Ferrara of Emilia-Romagna High Technology Network. Dr. Valentina Costa from the University of Ferrara is acknowledged for technical support. Dr. Daniela Palmeri from the University of Ferrara is acknowledged for SEM measurements.

7. Appendix A. Supplementary data

Supplementary information as noted in the text.

8. Figures and Tables

Figure 1. van Deemter plots showing the plate height, H, vs. the interstitial linear velocity, u_e, for Titan C_{18} 80Å (top) and 120Å (bottom) columns. Experimental data: nitrobenzene (cyan), toluene (orange), ethylbenzene (green), butylbenzene (purple). The maximum u_e corresponds to a flow rate F_v = 1.5 mL/min for the Titan C_{18} 80Å column (system back-pressure: 945 bar; column back-pressure: 764 bar) and 1.3 mL/min for the Titan C_{18} 120Å one (system back-pressure: 829 bar; column back-pressure: 673 bar). (For interpretation of references to colours in this figure, readers are referred to the web version of the article).

Figure 2. Chromatogram showing the separation of a mixture of benzene derivatives on the Titan C_{18} 80Å column. Flow rate: 1.0 mL/min. Mobile phase: ACN/water 60:40, v/v; T=35°C. Compounds: 1. Uracil (255980 N/m); 2. Phenol (283000, $k = 0.7$); 3. Benzaldheyde (289160 N/m, $k = 1.3$); 4. Nitrobenzene (291850 N/m, $k = 1.9$); 5. Benzene (280660 N/m, $k = 2.6$); 6. Toluene (279800 N/m, $k = 4.0$); 7. Ethylbenzene (264080 N/m, $k = 5.9$); 8. Propylbenzene (251060 N/m, $k = 9.4$); 9. Butylbenzene (241010 N/m, $k = 15.1$); 10. Pentylbenzene (230270 N/m, $k = 24.1$). The retention factor k was calculated by using uracil as the void time marker.

Figure 3. Chromatogram showing the separation of a mixture of benzene derivatives on the Titan C_{18} 120Å column. Flow rate: 1.1 mL/min. Mobile phase: ACN/water 60:40, v/v; T=35°C. Compounds: 1. Uracil (235310 N/m); 2. Phenol (298700, $k = 0.4$); 3. Benzaldheyde (310320 N/m, $k = 1.0$); 4. Nitrobenzene (320320 N/m, $k = 1.6$); 5. Benzene (306722 N/m, $k = 2.3$); 6. Toluene (312330 N/m, $k = 3.7$); 7. Ethylbenzene (302840 N/m, $k = 5.6$); 8. Propylbenzene (288995 N/m, $k = 9.1$); 9. Butylbenzene (274270 N/m, $k = 14.8$); 10. Pentylbenzene (255640 N/m, $k = 24.0$). The retention factor k was calculated by using uracil as the void time marker.

Figure 4. d_{Sauter}-based (d_{Sauter} = 2.04) reduced van Deemter plots (h vs. ν) for Titan C_{18} 80Å (top) and 120Å (bottom) columns. Experimental points: nitrobenzene (cyan), toluene (orange), ethylbenzene (green), butylbenzene (purple). (For interpretation of references to colours in this figure, readers are referred to the web version of the article).

Figure 5. Normalized particle size distributions (from SEM images) of the Titan C_{18} material (d_p = 1.9 μm) (red dotted line), compared to that of some common fully porous and superficially porous particles: XBridge C_{18} (d_p = 3.5 μm) (■), ACE3 C_{18} (d_p = 3.0 μm) (●), Gemini NX C_{18} (d_p = 3.0 μm) (◆), Hypersil GOLD C_{18} (d_p = 3.0 μm) (▲), Kinetex Fused Core C_{18} (d_p = 2.6 μm) (□), HALO Fused Core C_{18} (d_p = 2.7 μm) (△) and Poroshell C_{18} (d_p = 2.7 μm) (○). Data adapted from [44].

Figure 6. Band broadening (spatial peak variance, σ_x^2) as a function of parking time, t_p. Compound: toluene; eluent: ACN/water 60:40 v/v %; T = 35°C; column: Titan C_{18} 80Å. Linear regression coefficient, $R^2 > 0.999$.

Figure 7. Comparison between average reduced eddy dispersion terms, $a(\nu)$, of Titan C_{18} 80Å (blue squares) and 120Å (red squares) columns. The average was calculated on the four compounds considered in this work. (For interpretation of references to colours in this figure, readers are referred to the web version of the article).

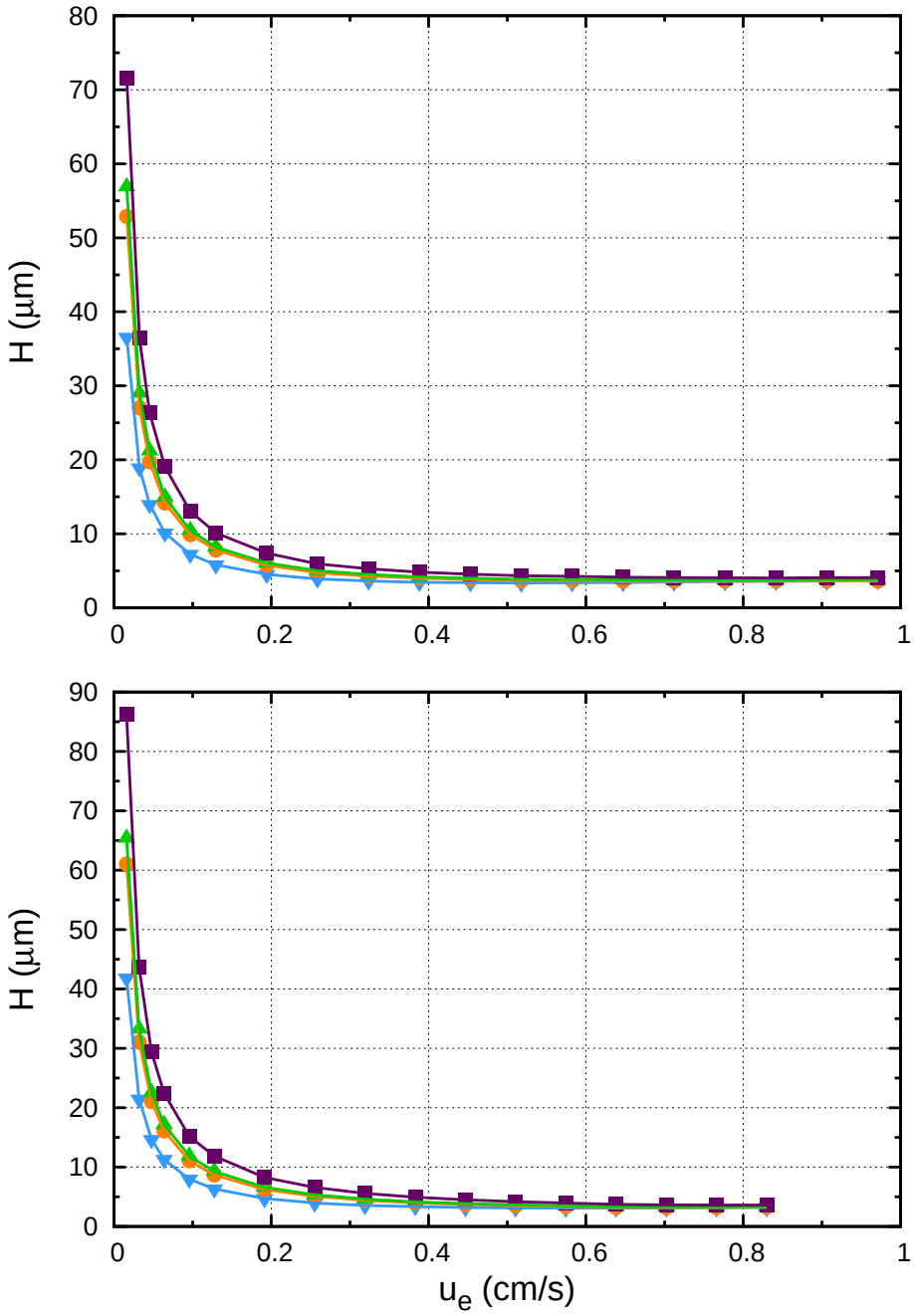
H (µm)
0
10
20
30
40
50
60
70
80
0
0.2
0.4
0.6
0.8
1
H (µm)
0
10
20
30
40
50
60
70
80
90
0
0.2
0.4
0.6
0.8
1
u_e (cm/s)

Figure 1:

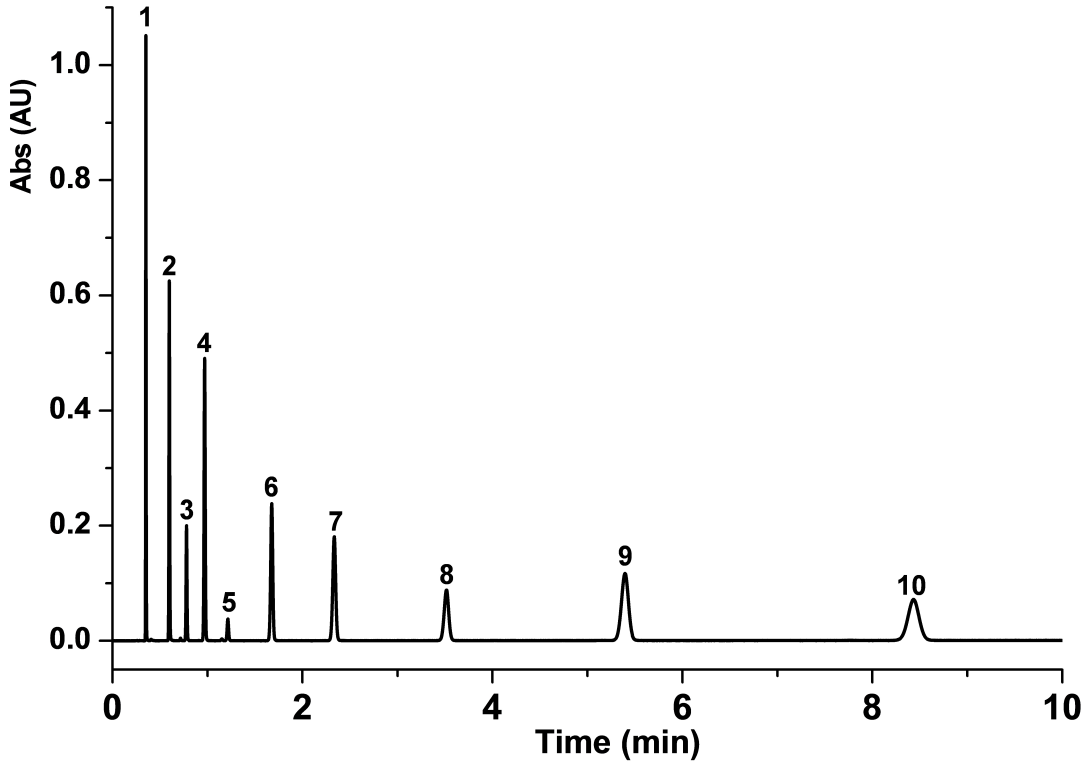

Figure 2:

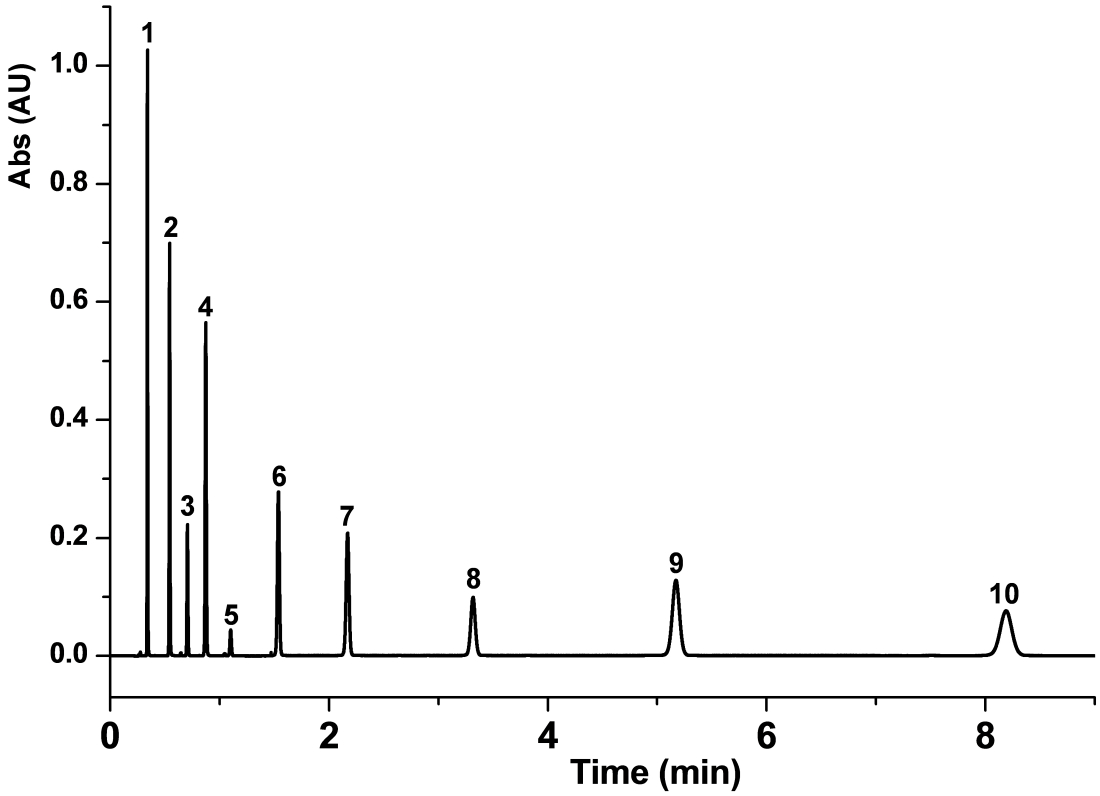

Figure 3:

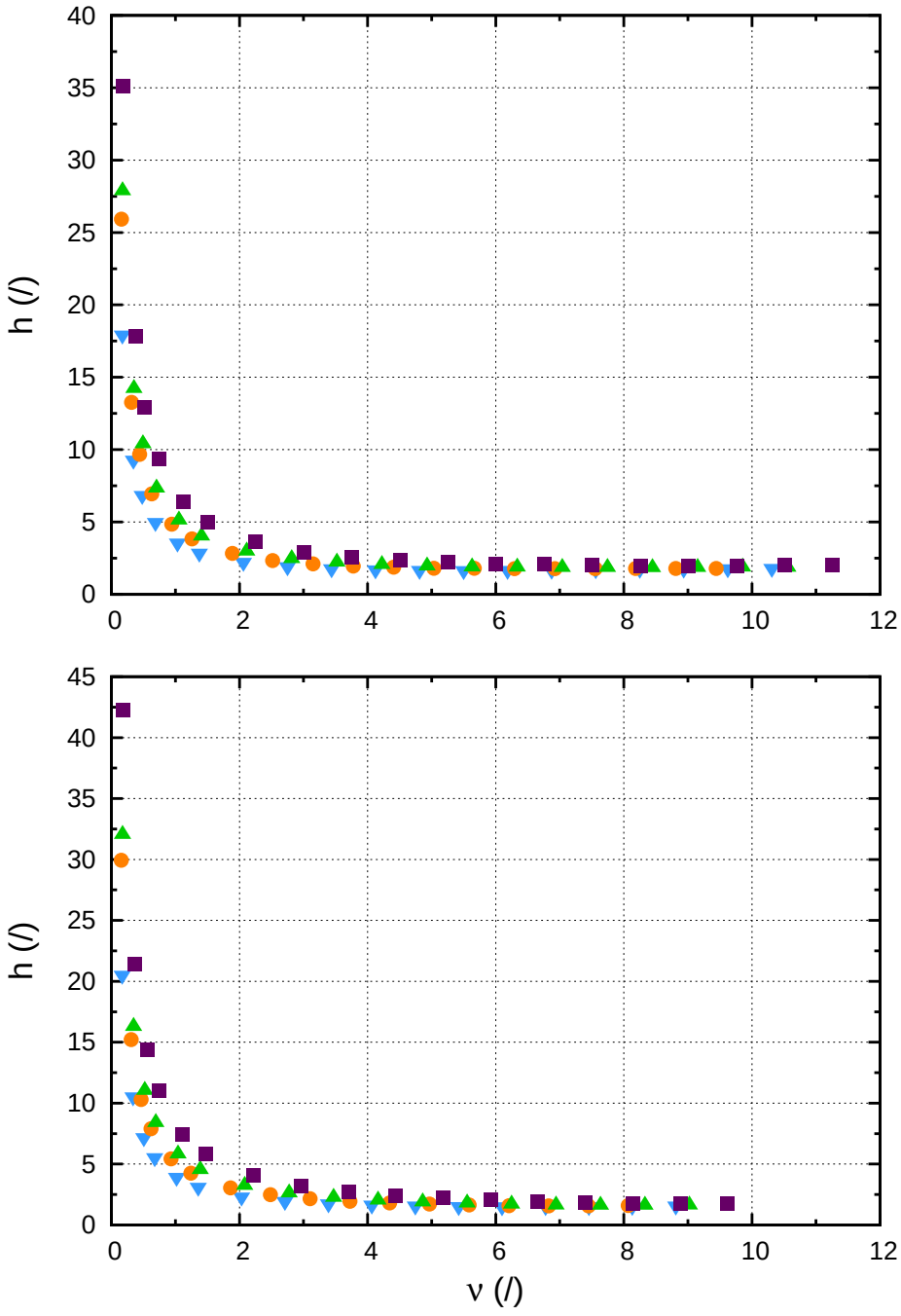

Figure 4:

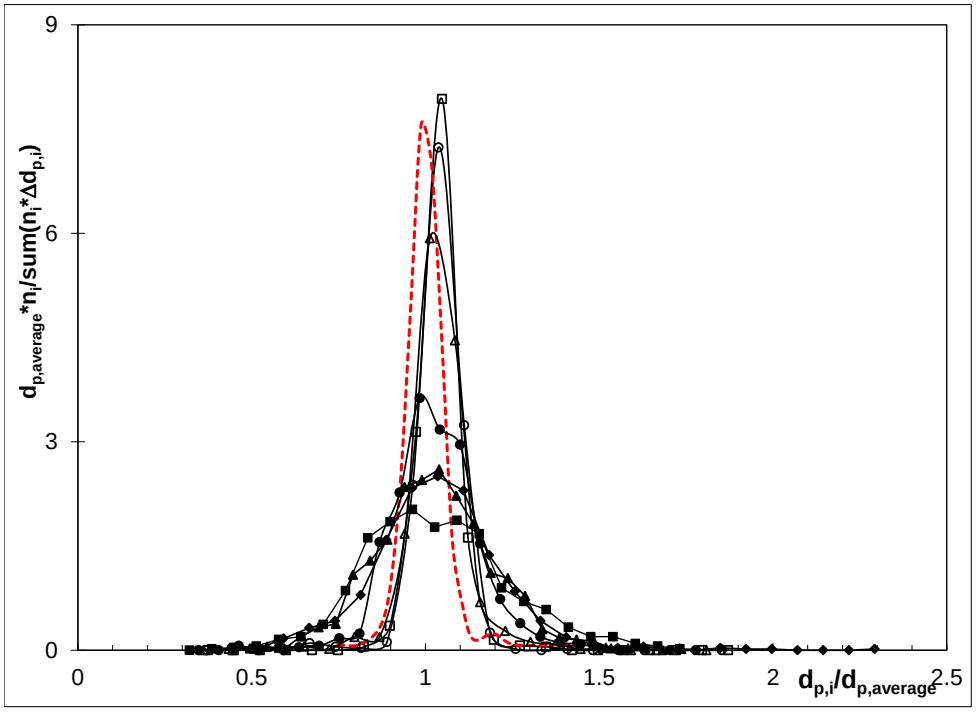

Figure 5:

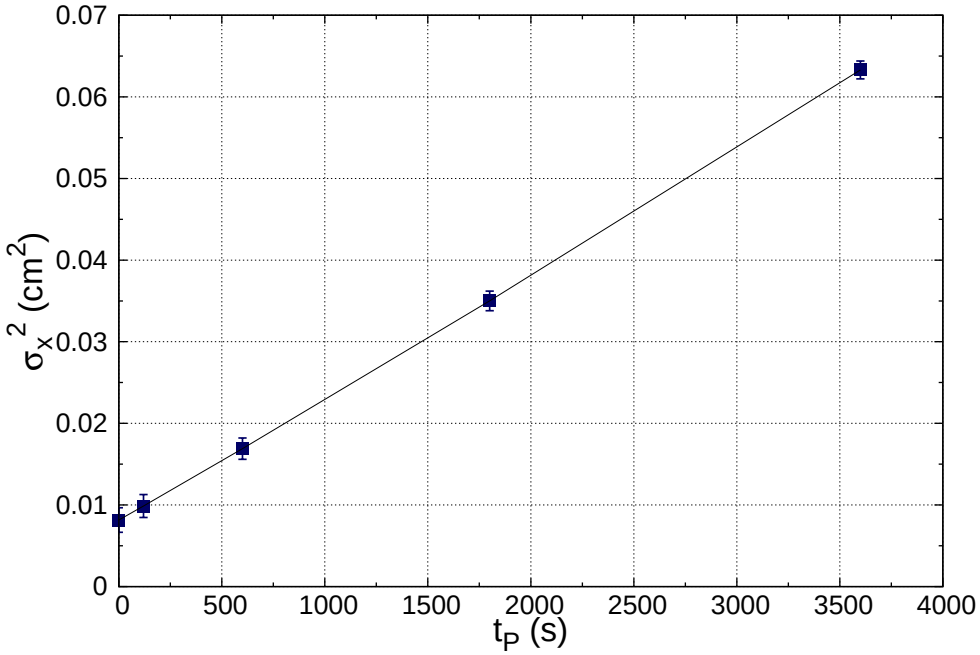
0.07
0.06
0.05
0.04
0.03
0.02
0.01
0
σ_x^2 (cm^2)
0
500
1000
1500
2000
2500
3000
3500
4000
t_P (s)

Figure 6:

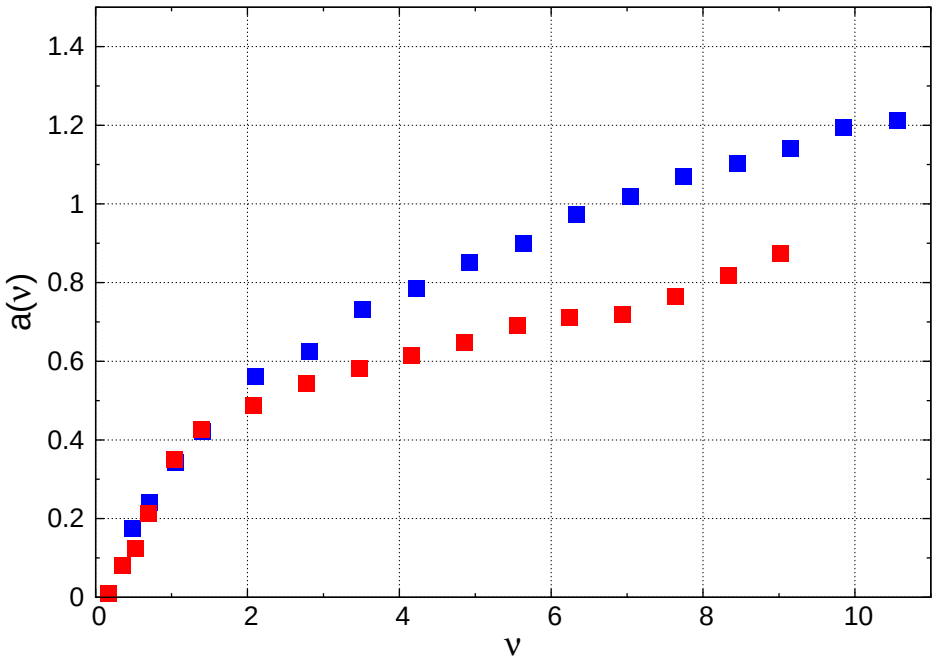

Figure 7:

Table 1: Geometrical characteristics and physico-chemical properties of Titan C_{18} columns: total (ϵ_t), interstitial (ϵ_e) and particle (ϵ_p) porosities; specific permeability (k_0); Kozeny-Carman constant (K_c). Batch: number of silica batch. Calculation of K_c for the Titan C_{18} columns was based on d_{Sauter}. See reference [1] for further details.

Column	Batch #	ϵ_{tot}	ϵ_e	ϵ_p	$k_0 \times 10^{11}$ (cm^2)	K_C
Titan-C_{18}, 80Å	7001	0.593	0.364	0.360	2.77	179
Titan-C_{18}, 120Å	2090	0.597	0.369	0.361	2.70	170

Table 2: Zone retention factor (k_1), retention factor (k), optimal reduced velocity (ν_{opt}), minimum reduced plate height (h_{min}) and reduced plate height at the maximum reduced velocity (ν_{max}) for the four compounds on the two Titan C_{18} columns.

	k_1		k		ν_{opt}		h_{min}		h (ν_{max})	
	80Å	120Å	80Å	120Å	80Å	120Å	80Å	120Å	80Å	120Å
Nitrobenzene	2.7	2.7	1.3	1.3	5.5	6.1	1.65	1.52	1.80 (10.3)	1.57 (8.8)
Toluene	5.6	5.6	3.1	3.1	6.3	6.8	1.78	1.57	1.79 (9.4)	1.59 (8.1)
Ethylbenzene	8.0	8.1	4.5	4.7	8.4	7.6	1.85	1.62	1.87 (10.6)	1.63 (9.0)
Butylbenzene	19.1	20.5	11.3	12.3	9.8	8.9	1.98	1.77	2.00 (11.3)	1.78 (9.6)

Table 3: Effective diffusion coefficient (D_{eff}), reduced longitudinal diffusion coefficient (b), relative permeability (α_{part}), whole-particle volume based equilibrium constant (K_p), overall diffusion coefficient through the porous particles (D_{part}) and mass transfer resistance across the stationary phase coefficient (c_s) for the four compounds in ACN/water 60:40 (v/v) at 35°C on Titan C_{18} columns.

	$D_{eff} \times 10^6$ (cm^2/s)		b		α_{part}		K_p		$D_{part} \times 10^6$ (cm^2/s)		c_s	
	80Å	120Å	80Å	120Å	80Å	120Å	80Å	120Å	80Å	120Å	80Å	120Å
Nitrobenzene	8.50	9.51	3.32	3.65	0.42	0.51	1.9	1.9	5.31	6.27	0.0244	0.0202
Toluene	6.85	7.64	4.31	4.78	0.67	0.82	4.4	4.5	4.42	5.27	0.0204	0.0171
Ethylbenzene	5.25	5.83	5.03	5.68	0.87	1.08	6.6	6.9	3.57	4.24	0.0173	0.0144
Butylbenzene	2.98	3.27	6.79	7.98	1.39	1.83	16.5	18.2	2.24	2.68	0.0124	0.0097

Table 4: Comparison between eddy dispersion values at $\nu \simeq 10$ between columns of different dimensions and particle diameters (d_p) packed with fully porous$^{(*)}$ (including Titan C_{18} 80Å and 120Å columns) and core-shell$^{(**)}$ particles. The last column reports literature reference from where the information was taken (JCA: Journal of Chromatography A).

Column	d_p	Length×I.D. (mm)	$a(\nu \sim 10)$	Ref.
Symmetry$^{(*)}$	5.0	150×4.6	1.30	JCA, 1355, 2014, 164 [3]
Luna$^{(*)}$	5.0	150×4.6	1.60	JCA, 1355, 2014, 179 [2]
Titan 80Å$^{(*)}$	1.9	100×3.0	1.20	this work
Titan 120Å$^{(*)}$	1.9	100×3.0	1.00	this work
Kinetex 1.7$^{(**)}$	1.7	100×4.6	1.80-1.90	JCA, 1355, 2014, 179 [2]
Kinetex 2.6$^{(**)}$	2.6	100×4.6	0.90-1.00	JCA, 1217, 2010, 1589 [48]

Bibliography

[1] O. H. Ismail, M. Catani, L. Pasti, A. Cavazzini, A. Ciogli, C. Villani, D. Kotoni, F. Gasparrini, D. S. Bell, Experimental evidence of the kinetic performance achievable with columns packed with the new 1.9 μm fully porous particles Titan c_{18}, J. Chromatogr. A, Submitted.

[2] F. Gritti, D. S. Bell, G. Guiochon, Particle size distribution and column efficiency. An ongoing debate revived with 1.9 μm Titan-C_{18} particles, J. Chromatogr. A 1355 (2014) 179–192.

[3] F. Gritti, G. Guiochon, The rationale for the optimum efficiency of columns packed with new 1.9μm fully porous Titan-C_{18} particles. A detailed investigation of the intra-particle diffusivity, J. Chromatogr. A 1355 (2014) 164–178.

[4] J. H. Knox, L. McLaren, New gas chromatographic method for measuring gaseous diffusion coefficients and obstructive factors, Anal. Chem. 36 (1964) 1477–1482.

[5] J. H. Knox, H. P. Scott, B and C terms in the van Deemter equation for liquid chromatography, J. Chromatogr. 282 (1983) 297–313.

[6] K. Miyabe, Y. Matsumoto, G. Guiochon, Peak parking-moment analysis. A strategy for the study of the mass-transfer kinetics in the stationary phase, Anal. Chem. 79 (2007) 1970–1982.

[7] K. Miyabe, N. Ando, G. Guiochon, Peak parking method for measurement of molecular diffusivity in liquid phase systems, J. Chromatogr. A 1216 (2009) 4377–4382.

[8] D. Cabooter, F. Lynen, P. Sandra, G. Desmet, Total pore blocking as an alternative method for the on-column determination of the external porosity of packed and monolithic reversed-phase columns, J. Chromatogr. A 1157 (2007) 131–141.

[9] A. Liekens, D. Cabooter, J. Denayer, G. Desmet, A study of the parameters affecting the accuracy of the total pore blocking method, J. Chromatogr. A 1217 (2010) 6754–6761.

[10] G. Desmet, K. Broeckhoven, J. De Smet, S. Deridder, G. V. Baron, P. Gzil, Errors involved in the existing B-term expressions for the longitudinal diffusion in fully porous chromatographic media. Part I: Computational data in ordered pillar arrays and effective medium theory, J. Chromatogr. A 1188 (2008) 171–188.

[11] K. Broeckhoven, D. Cabooter, F. Lynen, P. Sandra, G. Desmet, Errors involved in the existing B-term expressions for the longitudinal diffusion in fully porous chromatographic media. Part II: Experimental data in packed columns and surface diffusion measurements, J. Chromatogr. A 1188 (2008) 189–198.

[12] A. Liekens, J. Denayer, G. Desmet, Experimental investigation of the difference in b-term dominated band broadening between fully porous and porous-shell particles for liquid chromatography using the Effective Medium Theory, J. Chromatogr. A 1218 (2011) 4406–4416.

[13] J. C. Giddings, Dynamics of Chromatography, Marcel Dekker, New York, 1965.

[14] D. De Wilde, F. Detobel, J. Deconinck, G. Desmet, A numerical study of the assumptions underlying the calculation of the stationary zone mass transfer coefficient in the general plate height model of chromatography in two-dimensional pillar arrays, J. Chromatogr. A 1217 (2010) 1942–1949.

[15] F. Gritti, G. Guiochon, Mass transfer kinetics, band broadening and column efficiency, J. Chromatogr. A 1221 (2012) 2–40.

[16] G. Desmet, K. Broeckhoven, Equivalence of the different Cm- and Cs-term expressions used in Liquid Chromatography and a geometrical model uniting them, Anal. Chem. 80 (2008) 8076–8088.

[17] U. D. Neue, HPLC Columns: Theory, Technology and Practice, Wiley-VCH, 1997.

[18] C. Horváth, H. J. Lin, Band spreading in liquid chromatography: General plate height equation and a method for the evaluation of the individual plate height contributions, J. Chromatogr. 149 (1978) 43–70.

[19] H. Poppe, J. C. Kraak, J. F. K. Huber, J. H. M. v. Berg, Temperature gradients in HPLC columns due to viscous heat dissipation 14 (1981) 515–523.

[20] I. Halász, R. Endele, J. Asshauer, Ultimate limits in high-pressure liquid chromatography, J. Chromatogr. 112 (1975) 37–60.

[21] A. de Villiers, H. Lauer, R. Szucs, S. Goodall, P. Sandra, Influence of frictional heating on temperature gradients in ultra-high-pressure liquid chromatography on 2.1 mm i.d. columns, J. Chromatogr. A 1113 (2006) 84–91.

[22] G. Desmet, D. Cabooter, K. Broeckhoven, Graphical data representation methods to assess the quality of LC columns, Anal. Chem. 87 (2015) 8593–8602.

[23] J. H. Knox, Practical aspects of LC theory, J. Chromatogr. Sci 15 (1977) 352–364.

[24] R. W. Stout, J. J. DeStefano, L. R. Snyder, High-performance liquid chromatographic column efficiency as a function of particle composition and geometry and capacity factor, J. Chromatogr. 282 (1983) 263–286.

[25] F. Gritti, G. Guiochon, General HETP equation for the study of mass-transfer mechanisms in RPLC, Anal. Chem. 78 (2006) 5392–5347.

[26] H. T. Davis, The effective medium theory of diffusion in composite media, J. Am. Ceram. Soc. 60 (1977) 499–501.

[27] M. Barrande, R. Bouchet, R. Denoyel, Tortuosity of porous particles, Anal. Chem. 79 (2007) 9115–9121.

[28] G. Desmet, S. Deridder, Effective medium theory expressions for the effective diffusion in chromatographic beds filled with porous, non-porous and porous-shell particles and cylinders. Part I: Theory, J. Chromatogr. A 1218 (2011) 32–45.

[29] S. Deridder, G. Desmet, Effective medium theory expressions for the effective diffusion in chromatographic beds filled with porous, non-porous and porous-shell particles and cylinders. Part II: Numerical verification and quantitative effect of solid core on expected B-term band broadening, J. Chromatogr. A 1218 (2011) 46–56.

[30] A. Liekens, J. Billen, R. Sherant, H. Ritchie, J. Denayer, G. Desmet, High performance liquid chromatography column packings with deliberately broadened particle size distribution: Relation between column performance and packing structure, J. Chromatogr. A 1218 (2011) 6654–6662.

[31] S. Deridder, G. Desmet, New insights in the velocity dependency of the external mass transfer coefficient in 2D and 3D porous media for liquid chromatography, J. Chromatogr. A 1227 (2012) 194–202.

[32] G. Guiochon, A. Felinger, D. G. Shirazi, A. M. Katti, Fundamentals of Preparative and Nonlinear Chromatography, Academic Press, Elsevier, Second Edition, 2006.

[33] K. Miyabe, Y. Kawaguchi, G. Guiochon, Kinetic study on external mass transfer in high performance liquid chromatography system, J. Chromatogr. A 1217 (2010) 3053–3062.

[34] G. Desmet, S. Eeltink, Fundamentals for LC miniaturization, Anal. Chem. 85 (2013) 543–556.

[35] S. Bruns, T. Müllner, M. Kollmann, J. Schachtner, A. Höltzel, U. Tallarek, Confocal laser scanning microscopy method for quantitative characterization of silica monolith morphology, Anal. Chem. 82 (2010) 6569–6575.

[36] S. Bruns, U. Tallarek, Physical reconstruction of packed beds and their morphological analysis: Core-shell packings as an example, J. Chromatogr. A 1218 (2011) 1849–1860.

[37] D. Hlushkou, S. Bruns, U. Tallarek, High-performance computing of flow and transport in physically reconstructed silica monoliths, J. Chromatogr. A 1217 (2010) 3674–3682.

[38] S. Bruns, J. P. Grinias, L. E. Blue, J. W. Jorgenson, U. Tallarek, Morphology and separation efficiency of low-aspect-ratio capillary ultrahigh pressure liquid chromatography columns, Anal. Chem. 84 (2012) 4496–4503.

[39] D. Åsberg, J. Samuelsson, M. Lesko, A. Cavazzini, K. Kaczmarski, T. Fornstedt, Method transfer from high-pressure liquid chromatography to ultra-high-pressure liquid chromatography. II. Temperature and pressure effects, J. Chromatogr. A 1401 (2015) 52–59.

[40] I. Halász, K. Martin, Pore Size of Solids, Angew. Chem. Int. Ed. Engl 17 (1978) 901–908.

[41] F. Gritti, G. Guiochon, Impact of retention on trans-column velocity biases in packed columns, AICHE J. 56 (2010) 1495–1509.

[42] A. Felinger, Data analysis and signal processing in chromatography, Elsevier, Amsterdam, 1998.

[43] V. Baranau, U. Tallarek, Random-close packing limits for monodisperse and polydisperse hard spheres, Soft Matter 10 (2014) 3826–3841.

[44] D. Cabooter, A. Fanigliulo, G. Bellazzi, B. Allieri, A. Rottigni, G. Desmet, Relationship between the particle size distribution of commercial fully porous and superficially porous high-performance liquid chromatography column packings and their chromatographic performance, J. Chromatogr. A 1217 (2010) 7074–7081.

[45] F. Gritti, A. Cavazzini, N. Marchetti, G. Guiochon, Comparison between the efficiencies of columns packed with fully and partially porous C18-bonded silica materials, J. Chromatogr. A 1157 (2007) 289–303.

[46] F. Gritti, G. Guiochon, The quantitative impact of the mesopore size on the mass transfer mechanism of the new 1.9 m fully porous Titan-C_{18} particles. I: Analysis of small molecules, J. Chromatogr. A 1384 (2015) 76–87.

[47] A. Andrés, K. Broeckhoven, G. Desmet, Methods for the experimental characterization and analysis of the efficiency and speed of chromatographic columns: a step-by-step tutorial, Anal. Chim. Acta 894 (2015) 20–34.

[48] F. Gritti, I. Leonardis, D. Shock, P. Stevenson, A. Shalliker, G. Guiochon, Performance of columns packed with the new shell particles Kinetex-C_{18}, J. Chromatogr. A 1217 (2010) 1589–1603.

[49] H. Song, G. Desmet, D. Cabooter, Evaluation of the kinetic performance differences between Hydrophilic-Interaction Liquid Chromatography and Reversed-Phase Liquid Chromatography under conditions of identical packing structure, Anal. Chem. 87 (2015) 12331–12339.

Electronic Supplementary Material (online publication only)

Click here to download Electronic Supplementary Material (online publication only): suppl_material2.pdf

LaTeX Source Files

Click here to download LaTeX Source Files: paper2.tgz